

# Quantum-chromodynamic analysis of $eN$ deep-inelastic scattering data

L. F. Abbott

*Physics Department, Brandeis University, Waltham, Massachusetts 02154*

W. B. Atwood and R. Michael Barnett

*Stanford Linear Accelerator Center, Stanford University, Stanford, California 94305*

(Received 3 December 1979)

In the context of quantum chromodynamics (QCD), an analysis is presented of a compilation of  $eN$  deep-inelastic scattering data taken at SLAC. Included are data for  $F_2^p$ ,  $F_2^d$ ,  $F_2^p - F_2^d$ , and  $R$ . The interaction between the logarithmic scaling violation from  $\alpha_s$  and the power-law scaling violation from higher-twist terms is discussed. This interaction can affect the determination of the parameter  $\Lambda$  and can alter the predictions for the ratios of anomalous dimensions. Furthermore, we show that, in the context of QCD, higher-twist terms may be able to account for the observed value of  $R = \sigma_L/\sigma_T$  which appears to be anomalously large. Different experiments have made different assumptions for the value of  $R$  used in extracting  $F_2$  from their data. We show that these differences can account for the discrepancies in the relative normalizations of  $F_2$  from these experiments and also can have a significant effect on the value of  $\Lambda$  obtained.

## I. INTRODUCTION

It is widely believed that quantum chromodynamics<sup>1</sup> (QCD) is the correct theory of the strong interactions. This belief seems to be supported<sup>2,3</sup> by the good agreement between the scaling violations observed in deep-inelastic scattering and the logarithmic scaling violations predicted by QCD. However, QCD also predicts power-law violations coming from higher-twist operators<sup>4</sup> in the operator-product expansion. The resulting combination of power-law and logarithmic  $Q^2$  dependences can introduce uncertainties into the determination of the strong-coupling scale parameter  $\Lambda$ , and can alter the leading-twist predictions for the ratios of anomalous dimensions.<sup>2</sup> It is essential, therefore, to determine how much of the scaling violation seen in present experiments is due to the logarithmic variation of the coupling constant and how much is due to higher-twist effects before conclusions about the validity of QCD can be reached.

Since at present our ability to calculate or estimate higher-twist terms in QCD is quite limited, it is important to use experimental information to try to evaluate the contribution of higher-twist terms. This requires precise data over a very large range of  $Q^2$  values, and at each  $Q^2$ , a large range of  $x$  values is needed. Such data do not currently exist and even in the near future it may be necessary to combine data from different experiments. Since the Stanford Linear Accelerator Center (SLAC)  $eN$  data<sup>5</sup> are very precise, they can have an important impact on the analysis of QCD. In this paper we consider SLAC deep-inelastic scattering data for  $F_2^{eN}$  (from the process  $eN \rightarrow e + \text{anything}$ ) with  $Q^2 > 4 \text{ GeV}^2$  (for moments)

or  $Q^2 > 5 \text{ GeV}^2$  (for  $F_2$  evolution), taken by the SLAC and Massachusetts Institute of Technology (MIT) collaborations. These data were derived from a compilation of electroproduction data taken at SLAC, and include data for  $F_2^{ep}$ ,  $F_2^{ed}$ , and  $F_2^{ep} - F_2^{ed}$ .  $F_2^{ed}$  is purely flavor singlet,  $F_2^{ep} - F_2^{ed}$  is nonsinglet, and  $F_2^{ep}$  is a mixture. We limit ourselves to high  $Q^2$  and high  $W$  ( $W > 2 \text{ GeV}$ ) in order to minimize the impact of higher-twist terms<sup>2</sup> and of higher-order-in- $\alpha_s$  corrections<sup>6</sup> (which can be substantial<sup>7</sup> for  $Q^2 < 5 \text{ GeV}^2$ ).

When we consider the moments of  $F_2$  we apply only the  $Q^2$  cut, and we use the Nachtmann form<sup>8</sup> of the moments. By using the Nachtmann moments, or equivalently, the  $\xi$  variable of Georgi and Politzer<sup>8</sup> and by including the low- $W$  (resonance region) data and elastics, we are invoking the "local duality" hypothesis.<sup>9</sup>

With the present data, it is certainly advantageous to use the Altarelli-Parisi evolution equations<sup>10</sup> so that one can exclude the low- $W$  region, avoid unnecessary extrapolations, and make full use of low- and high- $x$  data. Even with the  $Q^2 > 5 \text{ GeV}^2$  cut, the results are quite sensitive to  $1/Q^2$  or  $1/Q^4$  higher-twist terms. Higher-twist terms reflect coherent phenomena such as transverse-momentum effects, diquark scattering, elastic scattering, resonance production, etc. Such terms must, of course, be present in any theory of the strong interactions. With or without higher-twist terms, QCD is consistent with almost all data. There is a notable exception: The leading-twist prediction<sup>11</sup> of QCD for the ratio  $R$  of longitudinal to transverse cross sections in deep-inelastic scattering is consistently much smaller than the SLAC data.<sup>12</sup> Here we will show that there is a possibility that the inclusion of higher-

twist terms will allow QCD to account for the  $R$  data.

## II. ANALYSIS OF SLAC DATA

The data used in the analysis of  $F_2^{eN}$  were derived from a compilation of electroproduction data<sup>5</sup> taken at SLAC. Details of the various experiments contributing to this data set are available elsewhere and will not be discussed here. The use of high- $Q^2$  data ( $Q^2 > 4$  or  $5 \text{ GeV}^2$ ) resulted in the elimination of all data for which the scattering angle was less than  $10^\circ$ . In addition, a cut on  $W$ , the invariant mass of the final hadronic state, was made on data used for fitting  $F_2$  directly. This cut required  $W > 2 \text{ GeV}$ . However, in the moment analysis, all data down to the one-pion threshold were used (with elastics also included).

The measured cross sections are mixtures of the  $F_1$  and  $F_2$  structure functions, and in the one-photon-exchange approximation can be written as

$$\frac{d\sigma}{dQ^2 dx} = \frac{4\pi\alpha^2}{Q^4} \left[ \left(1 - y - \frac{Mxy}{2E}\right) \frac{F_2(x, Q^2)}{x} + y^2 F_1(x, Q^2) \right]. \quad (2.1)$$

$M$  is the nucleon mass,  $E$  is the incident electron energy,  $y$  is the fractional energy loss of the electron [ $y = (E - E')/E$ , where  $E'$  is the energy of the scattered electron],  $Q^2 = 4EE' \sin^2(\theta/2)$ , where  $\theta$  is the scattering angle, and  $x$  is the Bjorken scaling variable ( $x = Q^2/2MyE$ ). The separation of the  $F_1$  and  $F_2$  contributions requires data at fixed  $x$  and  $Q^2$  for various values of  $y$ . Such analyses have been performed<sup>12</sup> but limit the kinematic range of the data. The approach used here was to separate out the  $F_2$  contribution by assuming the ratio of the longitudinal to transverse total photoabsorption cross sections  $R$  to be constant and equal to 0.21 as measured over a somewhat reduced kinematic range.<sup>12</sup> Explicitly (for  $e$ ,  $\mu$ , and  $\nu$  scattering),

$$\begin{aligned} \frac{2xF_1}{F_2} &= \left(1 + \frac{Q^2}{y^2 E^2}\right) / (1 + R) \\ &= \left(1 + \frac{4M^2 x^2}{Q^2}\right) / (1 + R). \end{aligned} \quad (2.2)$$

The procedure of assuming some value for  $R$  in order to extract  $F_2$  is also used by both neutrino<sup>13</sup> and muon<sup>14</sup> analyses since they also do not have sufficient data of good accuracy to make model-independent structure-function extractions. While  $R = 0.21$  has been used for  $eN$  data, the neutrino and muon experiments have often assumed the Callan-Gross relation<sup>15</sup>  $2xF_1 = F_2$  which implies  $R = 4M^2 x^2 / Q^2$ . Leading-twist QCD predicts that  $R$  should be small and should decrease as  $Q^2$  increases and as  $x$  increases. However, there is

no evidence for this behavior in the SLAC data (or other data), and (as discussed later) higher-twist terms could significantly change the expected magnitude and  $x$  dependence of the QCD prediction for  $R$ .

It is important to recognize that the assumption for  $R$  can have a significant effect on both the overall normalization and the  $Q^2$  dependence of the resulting  $F_2$ . We have analyzed the SLAC data with  $R = 0.21$ ,  $R = 0$ , and  $R = 4M^2 x^2 / Q^2$ . The latter two assumptions (which are not consistent with the SLAC data) decrease the overall normalization of  $F_2$  by 5 to 10% relative to the first assumption (for most  $x$  and  $Q^2$ ). At fixed  $Q^2$ , the differences are greatest at low  $x$ . At fixed  $x$ , the differences are greatest at high  $Q^2$  (but at high  $Q^2$ , only high- $x$  data exist). The different assumptions for  $R$  may account for relative normalization differences between different experiments. The impact on the  $Q^2$  dependence of  $F_2$  can be seen by noting that  $\Lambda(R = 0) - \Lambda(R = 0.21) \approx 140 \text{ MeV}$  and  $\Lambda(R = 4M^2 x^2 / Q^2) - \Lambda(R = 0.21) \approx 210 \text{ MeV}$  for the SLAC data.

The  $F_2$  structure functions were extracted from the cross-section data for both hydrogen and deuterium data. This set of structure functions consisted of about 2000 data points. There are small differences in normalization of the data at each angle for each experiment. To account for these systematic differences, the values of  $F_2$  were fit to an analytic form (not QCD) that represented the entire data set well. For each experiment in the data set and for each angle for which data were taken, the weighted ratio of the fitted model to the data was formed. The weighted ratios were used to correct the data at each angle for each experiment. The normalizations were found to be the same for both the hydrogen and the deuterium data, and the largest correction made was 4% but usually was 1–2%.

The data were binned into grids of  $x$  and  $Q^2$  for the  $F_2$  and moment analyses. Each data point falling inside a particular bin was corrected to the center of the bin using the aforementioned global fit. The data were then combined to give a single value for the structure function at the bin's center.

Typically, 15–20 data points fell into each bin. As such, the statistical errors tended to become very small (typically  $< 1\%$ ). A 4% error was added in quadrature to the statistical error for each grid point to account for systematic errors. Imposing this error after combining the data we believe more accurately represents the true experimental uncertainties.

Values for the neutron structure function were obtained by taking differences of the deuterium and hydrogen  $F_2$ 's. Fermi-motion effects were ac-

counted for using the procedure of Atwood and West<sup>16</sup> taking into account the corrections due to Frankfurt and Strikman.<sup>17</sup> The influence of Fermi motion on the results was in general found to be small as it only significantly affects the data with  $x > 0.8$ . The Frankfurt-Strikman modifications were small corrections to the Atwood and West approach, the largest being 7% at  $x = 0.88$ , and consequently they had no influence on the results.

### III. THE $F_2$ STRUCTURE FUNCTION

The  $F_2$  structure functions measured in deep-inelastic electroproduction can be written in terms of singlet and nonsinglet quark distribution functions as

$$F_2^{ep} = \frac{5}{18} F_2^S + \frac{3}{18} F_2^{NS}, \quad (3.1)$$

$$F_2^{ed} = \frac{5}{9} F_2^S, \quad (3.2)$$

$$E_2^{ep} - F_2^{en} = \frac{1}{3} F_2^{NS}, \quad (3.3)$$

where, if we ignore the small (few percent) effects of strange and charmed quarks,

$$F_2^S = x[u(x) + \bar{u}(x) + d(x) + \bar{d}(x)] \quad (3.4)$$

and

$$F_2^{NS} = x[u(x) + \bar{u}(x) - d(x) - \bar{d}(x)]. \quad (3.5)$$

Defining a gluon distribution function  $G$  analogous to the quark distribution functions of Eqs. (3.4) and (3.5), the  $Q^2$  evolution of the leading-twist contribution to  $F_2$  is predicted in lowest-order QCD by the following differential equations:

$$Q^2 \frac{\partial}{\partial Q^2} F_2^{NS}(x, Q^2) = \frac{\alpha_s(Q^2)}{3\pi} \left\{ [3 + 4 \ln(1-x)] F_2^{NS}(x, Q^2) + \int_x^1 dw \frac{2}{(1-w)} [(1+w^2) F_2^{NS}(x/w, Q^2) - 2F_2^{NS}(x, Q^2)] \right\}, \quad (3.6)$$

$$Q^2 \frac{\partial}{\partial Q^2} F_2^S(x, Q^2) = \frac{\alpha_s(Q^2)}{3\pi} \left\{ [3 + 4 \ln(1-x)] F_2^S(x, Q^2) + \int_x^1 dw \left( \frac{2}{(1-w)} [(1+w^2) F_2^S(x/w, Q^2) - 2F_2^S(x, Q^2)] + \frac{3}{2} N_f [w^2 + (1-w)^2] G(x/w, Q^2) \right) \right\}, \quad (3.7)$$

and

$$Q^2 \frac{\partial}{\partial Q^2} G(x, Q^2) = \frac{3\alpha_s(Q^2)}{\pi} \left\{ \left( \frac{11}{12} - \frac{N_f}{18} + \ln(1-x) \right) G(x, Q^2) + \int_x^1 dw \left[ \frac{wG(x/w, Q^2) - G(x, Q^2)}{1-w} + \left( w(1-w) + \frac{1-w}{w} \right) G(x/w, Q^2) + \frac{2}{9} \left( \frac{1+(1-w)^2}{w} \right) F_2^S(x/w, Q^2) \right] \right\}, \quad (3.8)$$

where  $N_f$  is the number of quark flavors and

$$\alpha_s(Q^2) = \frac{12\pi}{(33 - 2N_f) \ln(Q^2/\Lambda^2)}. \quad (3.9)$$

The QCD predictions are modified<sup>9</sup> when the effects of the  $\xi$  variable<sup>8</sup> are included (as discussed later in this section). Equations (3.6)–(3.8) must be supplied with boundary conditions by choosing values for the various distribution functions at some reference point  $Q^2 = Q_0^2$ . We parametrize the initial distribution functions in the following manner:

$$F_2^{NS}(x, Q_0^2) = C_1 x^{C_2} (1-x)^{C_3}, \quad (3.10)$$

$$F_2^S(x, Q_0^2) = C_4 (1 + C_5 x) (1-x)^{C_6}, \quad (3.11)$$

$$G(x, Q_0^2) = A (1-x)^5, \quad (3.12)$$

where  $A$  is fixed by the momentum sum rule

$$\int_0^1 dx (F_2^S + G) = 1 \quad (3.13)$$

to be

$$A = 6 \left[ 1 - \frac{C_4}{1+C_6} - \frac{C_4 C_5 \Gamma(1+C_6)}{\Gamma(3+C_6)} \right]. \quad (3.14)$$

For  $Q^2 \neq Q_0^2$  the forms of Eqs. (3.10)–(3.12) (not just the  $C_i$ ) are modified.

The expression for the singlet quark distribution, (3.11), with  $C_5$  as a free parameter was found to give a significantly better fit to the data than the simpler form corresponding to  $C_5 = 0$ , and so was used throughout our analysis. We have chosen  $Q_0^2 = 30.5 \text{ GeV}^2$ , where  $Q_0^2$  is the reference value of  $Q^2$  where the initial forms Eqs. (3.10)–(3.12) apply. Our analysis is not sensitive to the value of  $Q_0^2$  chosen, and this value was only taken for convenience.

We have fixed the exponent of  $(1-x)$  in the gluon distribution, Eq. (3.12), to be 5 because we have found that it cannot be reliably determined from the present data. We have varied this exponent from 4 to 7 and found that this had very little effect on the results we are reporting. This may seem surprising in view of the precise results<sup>18</sup> reported previously for  $\int_0^1 dx F_2^S$  in Eq. (3.13). However, that result was obtained by using a very low  $Q^2$  cut ( $Q^2 \geq 1 \text{ GeV}^2$ ). Furthermore, perfect scaling was assumed so that data at all  $Q^2$  were combined in a single  $x$  distribution before integrating. Note that the range of  $x$  for which data exist changes significantly as a function of  $Q^2$ . If instead one obtains  $\int_0^1 dx F_2^S$  in  $Q^2$  bins, significant fractions of the integrals come from extrapolated points (50% error bars were assigned to extrapolated points). We obtained results for  $\int_0^1 dx F_2^S$  where we averaged the values obtained for  $Q^2 > 4 \text{ GeV}^2$  (a similar procedure was followed for  $Q^2 > 6 \text{ GeV}^2$ ). For these  $Q^2$  cuts, elastic scattering and the resonance region contribute negligibly to the momentum-sum-rule integrals. We found

$$\int_0^1 dx F_2^S = \begin{cases} 0.61 \pm 0.09, & Q^2 > 4 \text{ GeV}^2, \\ 0.65 \pm 0.15, & Q^2 > 6 \text{ GeV}^2, \end{cases} \quad (3.15)$$

so that

$$\frac{\int_0^1 dx G}{\int_0^1 dx F_2^S} = \begin{cases} 0.64_{-0.2}^{+0.3}, & Q^2 > 4 \text{ GeV}^2, \\ 0.54_{-0.3}^{+0.5}, & Q^2 > 6 \text{ GeV}^2. \end{cases} \quad (3.16)$$

For  $x \geq 0.1$ , the evolution of the distribution functions is smooth and well behaved. However, for  $x \lesssim 0.1$ , the gluon distribution can vary extremely rapidly with  $Q^2$  and in fact can become negative. This behavior is presumably due to the breakdown of perturbation theory in the low- $x$  region. In this region, the evolution of the gluon distribution is highly sensitive to the reference point,  $Q_0^2$ , and to the initial condition, Eq. (3.12), which are chosen. Because of these problems and because of the fact that the gluon distribution is not well determined by experiment, QCD predictions for small  $x$  are unreliable when gluons are involved. Thus, only if  $x > 0.1$  will we indicate QCD results in which gluons play a role.

In most experiments, the range in  $x$  for which there are statistically significant data changes radically as  $Q^2$  increases. As a result it is crucial that the  $x$  dependence be fit at all  $Q^2$  rather than only at some  $Q_0^2$ . In other words, the determination of  $\Lambda$  and  $C_i$  should be done simultaneously. This procedure makes the best use of all available data and ensures that the proper values of  $\Lambda$  and  $C_i$  are obtained.

The parameters  $C_1$ – $C_3$  and  $\Lambda$  in Eq. (3.10) are determined simultaneously by integrating Eq. (3.6) for the nonsinglet contribution with Eq. (3.10) as a boundary condition. The simultaneous variation of  $C_1$ – $C_3$  and  $\Lambda$  leads to the best fit to  $F_2^{ep} - F_2^{en}$  at all  $Q^2$  values.  $C_4$ – $C_6$  are then determined analogously from the data for  $F_2^{ep}$  using the same values for  $C_1$ – $C_3$  which were obtained from the fit to  $F_2^{ep} - F_2^{en}$ .  $\Lambda$  was again allowed to be a free parameter in the second fit, but the  $\Lambda$  values obtained from the two fits were in excellent agreement.

We have obtained excellent fits to the data for both  $Q^2 > 2 \text{ GeV}^2$  and  $Q^2 > 5 \text{ GeV}^2$ . A cut in the final-state hadronic mass,  $W > 2 \text{ GeV}$ , was used to eliminate resonances and elastic scattering contributions. Since, at this point, we are ignoring higher-twist effects, it is desirable to make these  $Q^2$  and  $W$  cuts as high as possible. Our fits for  $Q^2 > 5 \text{ GeV}^2$ ,  $W > 2 \text{ GeV}$  are shown in Figs. 1 and 2. The values of the parameters found in our fits are dependent on higher-twist effects, target-mass corrections, and the parametrizations used. For qualitative purposes, we show the parameters for the simplest case (with  $Q_0^2 = 30.5 \text{ GeV}^2$ ):

$$\begin{aligned} C_1 &= 0.591, \\ C_2 &= 0.853, \\ C_3 &= 2.68, \\ C_4 &= 1.85, \\ C_5 &= 1.004, \\ C_6 &= 3.14, \\ \Lambda &= 0.628 \text{ GeV}. \end{aligned} \quad (3.17)$$

Very similar results were obtained for  $F_2^{ed}$  with all parameters ( $C_4$ – $C_6$  and  $\Lambda$ ) consistent with parameters (3.17).

It has been suggested that  $F_2^{NS}$  should vanish as  $\sqrt{x}$  in the small- $x$  region, whereas Eqs. (3.10) and (3.17) suggest  $F_2^{NS} \sim x^{0.853}$  for small  $x$ . However, there are no SLAC data at low  $x$  and  $C_2$  is actually determined by data at intermediate  $x$  values so no contradiction between theory and experiment is implied by this result. Furthermore, if we replace Eq. (3.10) with  $F_2^{NS}(x, Q_0^2) = C_1 x^{C_2} (1-x)^{C_3} \times (1+C_7 x)$ , then we find  $C_2 = 0.46$ .

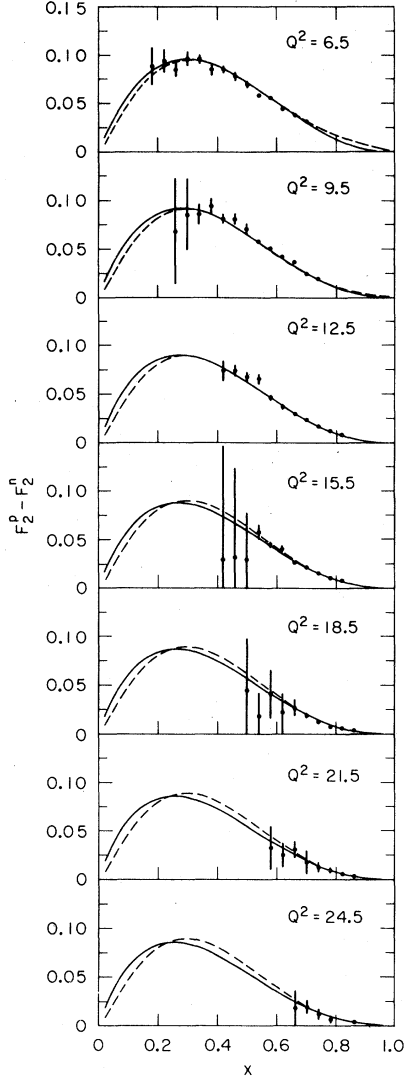


FIG. 1.  $F_2^p(x, Q^2) - F_2^n(x, Q^2)$  at various  $Q^2$  values. The solid curves are the QCD predictions; the dashed curves are described in the text. The data are from a compilation of SLAC-MIT data.<sup>5</sup>

Since we are using the lowest-order results of QCD the  $\Lambda$  given above should only be viewed as a parameter of the fit, and no physical significance should be attached to its specific value. In particular, the  $\Lambda$  value given in Eq. (3.17) should not be compared with  $\Lambda$ 's obtained from other experiments even as a consistency check. In addition, higher-twist effects could significantly change the value of  $\Lambda$  obtained from the data (see below).

There may be additional sources of significant scaling violation, even for  $Q^2 > 5 \text{ GeV}^2$  and  $W > 2 \text{ GeV}$ . These come from the nonleading twist operators in the operator-product expansion. It

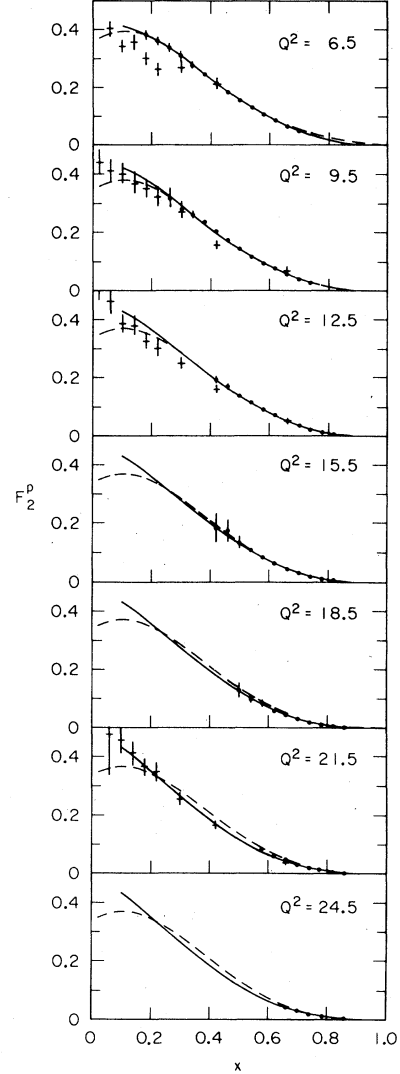


FIG. 2.  $F_2^p(x, Q^2)$  at various  $Q^2$  values. The solid curves are the QCD predictions; the dashed curves are described in the text. The fit was done using only SLAC-MIT data<sup>5</sup> (solid dots), but the Chicago-Harvard-Illinois-Oxford data<sup>14</sup> are also shown. The error bars are often smaller than the dots.

should be pointed out that the magnitude of the effects of these higher-twist operators depends on the detailed structure of the proton and cannot be determined by perturbative analysis of QCD. In Figs. 1 and 2 we have also shown that the effects of higher-twist terms on analyses of scaling violation could be quite drastic by considering the extreme case ( $\Lambda \approx 0$ ) in which *all* scaling violation comes from higher-twist effects. On the basis of this assumption we have obtained an excellent fit to the  $F_2$  data for  $Q^2 > 5 \text{ GeV}^2$ ,  $W > 2 \text{ GeV}$  as is shown by the dashed curves in Figs. 1 and 2. These fits are given by

$$F_2^{\text{NS}}(x, Q^2) = 1.2x^{1.2}(1-x)^3 \left[ 1 - \frac{0.4 \text{ GeV}^2}{(1-x)Q^2} + \frac{(1.7 \text{ GeV}^2)^2}{(1-x)^2 Q^4} \right], \quad (3.18)$$

$$F_2^{\text{S}}(x, Q^2) = 1.2(1+4.7x)(1-x)^{3.5} \left[ 1 - \frac{0.3 \text{ GeV}^2}{(1-x)Q^2} + \frac{(1.7 \text{ GeV}^2)^2}{(1-x)^2 Q^4} \right]. \quad (3.19)$$

Although there are no unequivocal calculations in QCD of the form of higher-twist terms, one can argue using the quark-counting approach,<sup>19</sup> that the above  $x$  and  $Q^2$  dependence of the higher-twist terms is reasonable.

Since either leading-twist terms with QCD or higher-twist effects alone can account for the data, it is not surprising that one cannot determine how much of the scaling violation is coming from the leading-twist terms and how much is coming from other sources. *Furthermore, higher-twist effects of even a modest size will allow almost any hypothetical alternative theory to fit the data.*

Even if higher-twist effects are set equal to zero one cannot unambiguously detect the key features of QCD in the data. For example, one can change the running coupling constant in Eqs. (3.6)–(3.8) to a constant independent of  $Q^2$  and obtain an excellent fit to the data. Thus, the logarithmic variation in  $Q^2$  typical of QCD has not been clearly detected. Similarly, since our results are insensitive to the gluon distribution being used, one cannot claim to see evidence of the effects of this distribution on scaling violation in the data.

We have noted that, at present, deep-inelastic data cannot distinguish the logarithmic variation of the leading-twist QCD prediction from the power-law scaling violations coming from higher-twist terms. However, the data can determine the relationship between these two forms of scaling violation. This is shown<sup>20</sup> in Fig. 3. We have modified the leading-twist QCD predictions of Eqs. (3.6)–(3.12) by including higher-twist terms of the following two forms<sup>19</sup>:

$$F_2 = F_2^{\text{QCD}} \left( 1 + \frac{\mu_1^2}{(1-x)Q^2} \right) \quad (i=1)$$

or

$$F_2 = F_2^{\text{QCD}} \left( 1 + \frac{\mu_2^4}{(1-x)^2 Q^4} \right) \quad (i=2). \quad (3.20)$$

The  $x$  dependence indicated here is suggested by quark-counting rules. In Fig. 3 we have plotted the parameter  $\mu_i$ , which indicates the magnitude

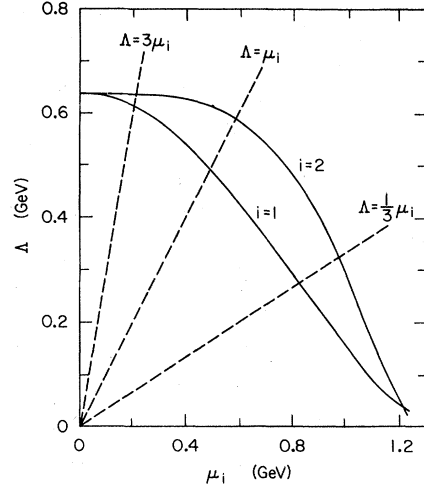


FIG. 3. The value of  $\Lambda$  obtained when higher-twist contributions have been assumed (Ref. 20).  $\mu_1$  and  $\mu_2$  indicate the magnitude of the higher-twist terms where the two forms considered are shown in Eq. (3.20).

of higher-twist effects versus  $\Lambda$ , which is a measure of the scaling violations in QCD. Both of the cases in Eq. (3.20) are displayed. These results were obtained by fixing the value of  $\Lambda$  and then determining the best value of  $\mu_i$  to fit the data. It is plausible that  $\Lambda$  may be reduced by as much as a factor of 2 or by as little as a few percent when the correct higher-twist terms are added.

The reason that higher-twist terms can have a large effect on QCD predictions at "high"  $Q^2$  is evident by considering Eqs. (3.20) and (5.9). If one assumes that  $\mu_1 \approx \Lambda \approx 0.5 \text{ GeV}$  for  $F_2$  (or  $a \approx \Lambda \approx 0.5 \text{ GeV}$  for moments), one finds that in the range  $Q^2 = 4\text{--}100 \text{ GeV}^2$ , typically about 35% of the scaling violation is due to the higher-twist term. Even for the range  $Q^2 = 10\text{--}100 \text{ GeV}^2$ , about 20% is due to the higher-twist term. Although the higher-twist term is small at these values of  $Q^2$ , it changes more rapidly with  $Q^2$ .

In Fig. 4, we have extrapolated the predictions for  $F_2^{\text{ep}}(x, Q^2)$  into the low- $W$  (high- $x$ ) region as indicated by the solid curve. The data clearly show the resonances which appear in this region. We have indicated the elastic scattering contribution (which is actually a  $\delta$  function at  $x=1$ ) by including one extra bin from  $x=1$  to  $x=1.04$ . The area under the data point in this bin is equal to the area under the elastic peak at  $x=1$ . The  $x$ -scaling QCD predictions for  $F_2(x, Q^2)$  undershoot the resonances and do not in any way account for the elastic-scattering contribution in the data. The dashed curve in these figures shows the  $\xi$ -scaling predictions<sup>9</sup>  $\tilde{F}_2(x, Q^2)$  obtained from the QCD predictions by writing

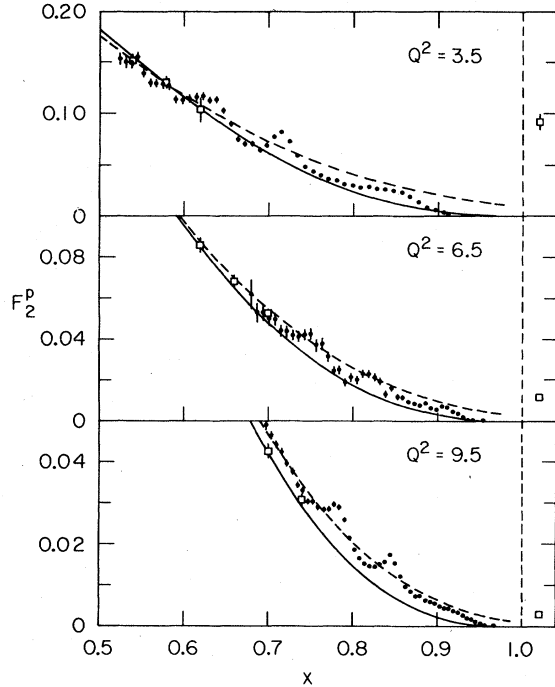


FIG. 4.  $F_2^p(x, Q^2)$  at small  $W$ . The solid (dashed) curve is the  $x$  ( $\xi$ ) scaling prediction of QCD. Elastics are shown in extra bins from  $x=1$  to 1.04 where the areas under the data points in these bins are equal to the areas under the elastic spikes at  $x=1$  in the original data. All data are from SLAC-MIT (Ref. 5). The square points have  $W > 2$  GeV and are a compilation of SLAC-MIT data. The dots indicate some of the data in the resonance region.

$$\begin{aligned} \tilde{F}_2(x, Q^2) = & \frac{x^2}{\xi^2} v^3 F_2(\xi, Q^2) + \frac{6M^2}{Q^2} x^3 v^4 \int_{\xi}^1 dx' \frac{F_2(x', Q^2)}{x'^2} \\ & + \frac{12M^4}{Q^4} x^4 v^5 \int_{\xi}^1 dx' \int_{x'}^1 dx'' \frac{F_2(x'', Q^2)}{x''^2}, \end{aligned} \quad (3.21)$$

where

$$\xi = \frac{2x}{1 + (1 + 4M^2 x^2 / Q^2)^{1/2}} \quad (3.22)$$

and

$$v \equiv \left(1 + \frac{4M^2 x^2}{Q^2}\right)^{-1/2}. \quad (3.23)$$

In generating  $\tilde{F}_2$  we have used the same parameters  $C_1$ - $C_6$  and  $\Lambda$  as in our  $x$ -scaling fits of QCD to the data. The  $\xi$ -scaling prediction is based on incorporating the target-mass condition  $p^2 = M^2$  into the basic QCD predictions. From Fig. 4, one can see that the  $\xi$ -scaling curve, on the average, agrees well with the resonance contributions and that the excess area under the  $\xi$ -scaling curve

near  $x=1$  is about equal to the area under the elastic peak as noted by De Rújula, Georgi, and Politzer.<sup>9</sup> Note that the  $\xi$ -scaling curve violates the kinematic bound  $F_2=0$  for  $x \geq 1$ . Remember that the correspondence between the  $\xi$ -scaling curve and the data from the resonance region is assumed when Nachtmann moments are used at low  $Q^2$ .

The threshold behavior in Eq. (3.21) is not correct. One method of dealing with this problem (see K. Bitar *et al.* in Ref. 4) is to replace the upper limits of integration (1) with  $\xi_{\max}(q^2)$ . However, this procedure seems ambiguous to us, and the form of the corrections which it induces are similar to the corrections in Eq. (3.20).

#### IV. THE RATIO OF LONGITUDINAL TO TRANSVERSE CROSS SECTIONS

In addition to  $F_2$ , QCD also makes a prediction for the longitudinal structure function in electroproduction. In the leading-twist approximation, and to lowest nontrivial order in  $\alpha_s$ , this is

$$\begin{aligned} F_L(x, Q^2) = & \frac{\alpha_s(Q^2)}{2\pi} x^2 \int_x^1 \frac{dw}{w^3} \left[ \frac{2}{3} F_2(w, Q^2) \right. \\ & \left. + \frac{10}{9} N_f (1-x/w) G(w, Q^2) \right]. \end{aligned} \quad (4.1)$$

For neutrino scattering, the number  $\frac{10}{9}$  in Eq. (4.1) is replaced with 4. From this, the ratio

$$R = \frac{F_L}{2xF_1} = \frac{F_L}{F_2} + O(\alpha_s^2) \quad (4.2)$$

can be predicted. Equations (4.1) and (4.2) ignore target-mass corrections of order  $M^2 x^2 / Q^2$ ; however, these can be taken into account by using the  $\xi$  variable.<sup>9</sup> Using our fits from  $F_2$  data, we have generated the solid curves in Fig. 5 which are shown for various  $Q^2$  values along with the SLAC-MIT data points.<sup>12</sup> Both systematic and statistical errors are shown. Most of the experimental error is due to what is considered a conservative estimate of systematic errors. As can be seen, the data disagree with the QCD predictions for  $x \geq 0.3$  although the effect of missing several data points is not cumulative since most of the experimental error is systematic. Thus, the QCD value is in disagreement at about a 1.5-2-standard-deviation level. The QCD curves in this figure correspond to  $Q^2 = 3, 6, 9, 12$ , and  $18 \text{ GeV}^2$  going from the top curve to the bottom curve.

In Ref. 21, the effect of a significant dynamical diquark substructure of the proton on deep-inelastic experiments was considered. This corresponds to the inclusion of higher-twist terms of order  $1/Q^2$  and  $1/Q^4$ . It was found<sup>21</sup> that diquark terms

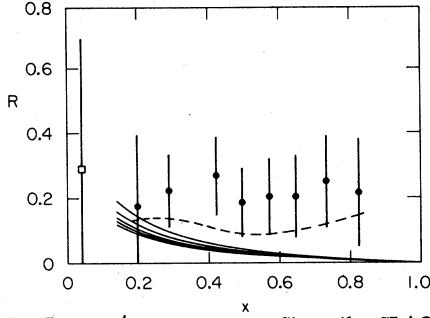


FIG. 5.  $R \equiv \sigma_L / \sigma_T$  versus  $x$ . Since the SLAC-MIT data (Ref. 12) show no evidence of  $Q^2$  dependence, in this figure all data have been combined; the error bars are mostly systematic. The solid curves show QCD with no higher-twist contributions for the  $Q^2$  values covered by the data. The dashed curve is QCD plus a diquark model (Ref. 21) of higher-twist contributions; the curve reflects the average  $Q^2$  of the data points through which it is drawn. The square point represents the high- $Q^2$  data of Anderson *et al.* (Ref. 14).

alone (without QCD) could account for both  $F_2$  and  $R$  data. We have included such higher-twist terms along with the leading-twist QCD predictions and obtained an excellent fit to  $F_2$  data. Of course, the value of  $\Lambda$  determined by this fit was smaller ( $\Lambda = 0.195$  GeV) than that obtained by fitting QCD with no higher-twist effects. Since the diquarks are bosons, they contribute strongly to  $R$  and, as is shown by the dashed curve in Fig. 5, large values of  $R$  can occur in this model for low  $Q^2$  or at large  $x$ . The dashed curve was obtained by computing  $R$  in each  $x$  bin using the average value of  $Q^2$  for that  $x$  bin. In Fig. 6 the data and predictions are broken down into  $Q^2$  bins. The resulting predictions in both figures are in rough, though not perfect, agreement with the data. This indicates that large values of  $R$  can occur through higher-twist effects which are completely consistent with other deep-inelastic data even within the framework of QCD.

#### V. MOMENTS OF $F_2^{ep} - F_2^{en}$

The moments of the nonsinglet part of the  $F_2$  structure functions have simple logarithmic dependences which are calculable in QCD. At large  $Q^2$ , leading-order QCD predicts

$$M_2^{NS}(i, Q^2) = \int_0^1 dx x^{i-2} (F_2^{ep} - F_2^{en}) \quad (5.1)$$

$$\propto (\ln Q^2 / \Lambda^2)^{-d_i}. \quad (5.2)$$

Therefore, one moment is related to another moment by a power equal to the ratio of the anomalous

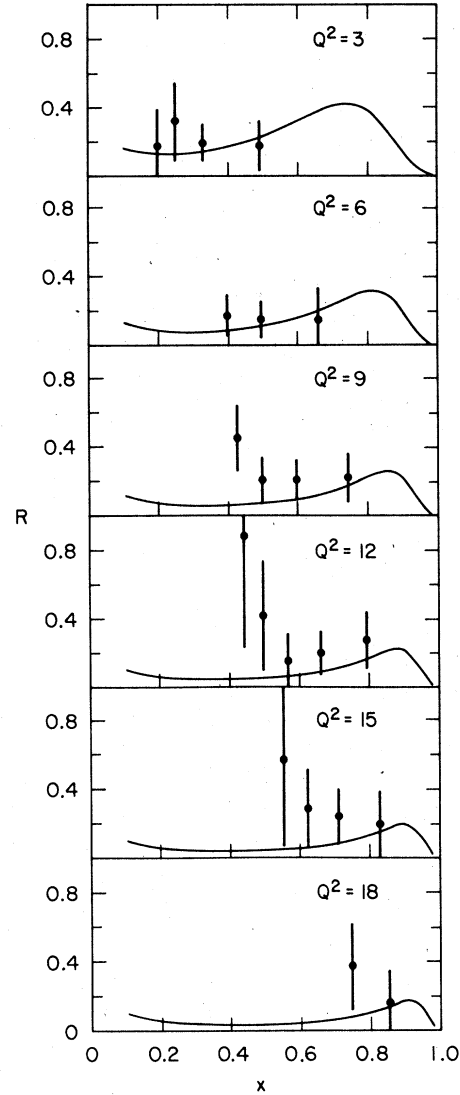


FIG. 6.  $R \equiv \sigma_L / \sigma_T$  at various  $Q^2$  values. The data are a compilation of all SLAC-MIT data (Ref. 12); the error bars are mostly systematic. The curves show the results of QCD when a higher-twist contribution from diquark scattering (using the model of Ref. 21) is added.

dimensions ( $d_i/d_j$ ) of the two moments:

$$M_2^{NS}(i, Q^2) = \text{constant} \times [M_2^{NS}(j, Q^2)]^{d_i/d_j}. \quad (5.3)$$

This ratio is independent of the number of quark flavors and of the magnitude of  $\Lambda$ . In practice, moment analyses contain other assumptions which become especially significant at low  $Q^2$ . The Nachtmann moments<sup>8</sup> account for the target-nucleon mass in deep-inelastic scattering. For the nonsinglet combination  $F_2^{ep} - F_2^{en}$  they are given by

$$M_2^{NS}(i, Q^2) = \int_0^1 dx \frac{\xi^{i+1} [(i^2 + 2i + 3) + 3(i+1)(1 + 4M^2 x^2 / Q^2)^{1/2} + i(i+2)(4M^2 x^2 / Q^2)]}{(i+2)(i+3)} [F_2^{ep} - F_2^{en}], \quad (5.4)$$



where

$$\xi = \frac{2x}{[1 + (1 + 4M^2x^2/Q^2)^{1/2}]} \quad (5.5)$$

$M_2^{ep}$  and  $M_2^{ed}$  are defined equivalently. The Nachtmann moments become equal to Eq. (5.1) at large  $Q^2$ . There are other effects (from higher-twist terms) which we do not know how to account for. For example, nothing in our formalism tells us that there is a minimum hadronic mass. One can use the difference between the two moments, Eqs. (5.1) and (5.4), as a *rough* estimate of unknown effects. In this way a value of  $Q^2$  below which uncertainties of this kind may become important can be approximately established. In Fig. 7, the  $N = 4$  moments for these two versions are plotted against  $Q^2$ . The ordinary moments rapidly become larger than the Nachtmann moments below  $Q^2 = 4 \text{ GeV}^2$ . For higher moments this "safe"  $Q^2$  is even larger. We choose to use the Nachtmann moments in this analysis but consider the extension of moment analyses below  $Q^2 = 4 \text{ GeV}^2$  to be unreliable.

The moment integrals cover the full  $x$  range from 0–1. The question of whether to include the elastic peak becomes important at low  $Q^2$  as it can give a large contribution to the moment integral. The fractional contribution of elastic scattering to the Nachtmann moments of  $F_2^{ep} - F_2^{en}$  is shown on Fig. 8 for  $n = 2, 5$ , and  $9$  as a function of  $Q^2$ . Higher moments such as  $5$  and  $9$  heavily weight the region near  $x = 1$  and thus acquire large elastic contributions. Again the data would suggest a  $Q^2$  minimum of at least  $4 \text{ GeV}^2$  be established in order to keep the elastic contribution small.

The next portion of the moment integral to be

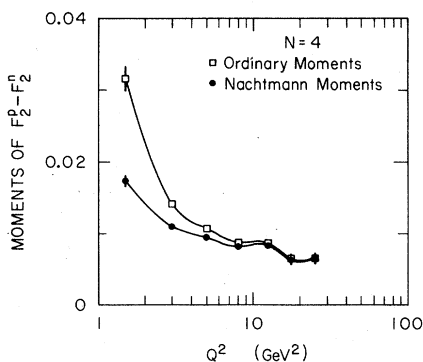


FIG. 7. A comparison of ordinary moments and Nachtmann moments from the SLAC-MIT data of Ref. 5. Curves are drawn connecting the data points to help guide the eye. Large target-mass effects are apparent for  $Q^2 \lesssim 4 \text{ GeV}^2$ .

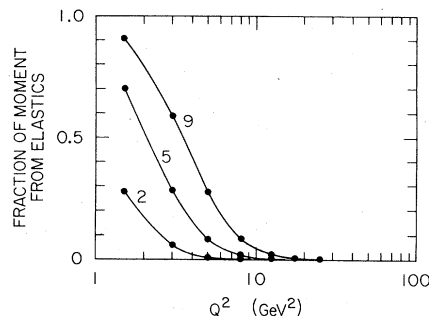


FIG. 8. The fraction of the Nachtmann moments (for  $i = 2, 5, 9$ ) which come from elastic scattering. The contributions at relatively large  $Q^2$  are still quite significant. The data are from Ref. 5 with error bars not shown.

concerned with is that part which lies inside the "resonance region" ( $W < 2 \text{ GeV}$ ). For these low values of  $W$ , distinct final states have been identified, and final-state interactions in the hadronic system are important. As such, one would want these contributions to the moments to be small. In Fig. 9 the fraction of the second, fifth, and ninth Nachtmann moments coming from both elastic scattering and resonance-region production is plotted against  $Q^2$ . The higher moments are seen to have large contributions from  $W < 2 \text{ GeV}$  even for  $Q^2$  in excess of  $10 \text{ GeV}^2$ .

All moments, except those calculated using hydrogen data, implicitly include Fermi-motion effects. These effects which are uncertain in size are large in the high- $x$  region. They are also largely independent of  $Q^2$ . As such, high moments could have this additional uncertainty. We investigated the ratio of the moments of  $(F_2^{ep} + F_2^{en})$  where Fermi motion effects have been accounted for<sup>16,17</sup> to moments of  $F_2^{ed}$ . This ratio was found to deviate from unity by a few percent and to have little  $Q^2$  dependence. As expected, the effect is

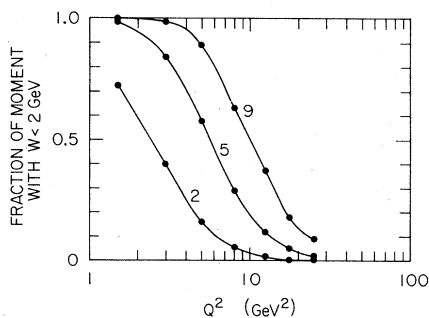


FIG. 9. The fraction of the Nachtmann moments (for  $i = 2, 5, 9$ ) which come from the resonance region ( $W < 2 \text{ GeV}$ ). The contributions at relatively large  $Q^2$  are still significant. The data are from Ref. 5 with error bars not shown.

largest for the higher moments. If we write

$$M_2^{ed}(i, Q^2) = K_i [M_2^{ep}(i, Q^2) + M_2^{en}(i, Q^2)], \quad (5.6)$$

then  $K_5 \approx 1.04$  and  $K_9 \approx 1.09$ . We conclude that Fermi-motion uncertainties are small compared with other uncertainties.

We have fitted the ratio of anomalous dimensions between various pairs of Nachtmann moments for  $F_2^{ep} - F_2^{en}$  with a proper accounting of the correlation of errors between moments. At each  $Q^2$  an analytic form normalized to the data (at that  $Q^2$ ) was used to obtain the values of  $F_2^{ep} - F_2^{en}$  for  $x$  bins where no data exist. A 50% error was assigned to extrapolated points. The results are shown in Fig. 10 along with the results from BEBC-Gargamelle neutrino data<sup>13</sup> for  $\chi F_3$ . In this figure

$$r_{ij} \equiv d_i/d_j. \quad (5.7)$$

The horizontal lines indicated the predictions of leading-order QCD. The shaded areas show a reasonable range for the second-order QCD predictions<sup>2</sup> which are not precisely defined and which have some  $Q^2$  dependence.

The Nachtmann moments have been used here. As an example of their impact on  $r_{ij}$ , we have used the QCD evolution equations to generate "data" for  $7 \leq Q^2 \leq 65 \text{ GeV}^2$  but *without* using the  $\xi$  variable. If one uses the standard moments [Eq. (5.1)] to analyze these data, then one obtains  $r_{53} = 1.46$  as expected. However, using Nachtmann moments one finds  $r_{53} = 1.23$ . The opposite is clearly true: If we generated data using the  $\xi$  formalism (thereby using the "local duality" argu-

ment of De Rújula-Georgi-Politzer<sup>9</sup> to account for elastic scattering and resonance production), we would obtain the correct  $r_{ij}$  only by using Nachtmann moments.

In Fig. 10 we have also shown the results of combining the  $\chi F_3$  neutrino data of the CERN-Dortmund-Heidelberg-Saclay (CDHS) collaboration<sup>13</sup> with the SLAC data for  $F_2^{ed}$ . The SLAC data are used *only* for  $x > 0.4$  where we assumed  $\frac{2}{5} F_2^{ed} = \chi F_3^{NN}$ . In bins where both groups had data, a weighted average was used. As for the other results on Fig. 10 we used an analytic form to extrapolate where no data existed and assigned 50% errors to extrapolated points. In this case that form was

$$\chi F_3 = C(Q^2) x^{\eta_1} (1-x)^{\eta_2}, \quad (5.8)$$

where<sup>13</sup>  $\eta_1 = 0.51$  and  $\eta_2 = 3.03$ .  $C(Q^2)$  was fit to available data at each  $Q^2$ . For comparison one could allow  $\eta_1$  and  $\eta_2$  to be given by the Buras-Gaemers form<sup>22</sup> and therefore  $Q^2$  dependent. (The Buras-Gaemers forms come from an approximate solution of QCD.) If we obtain  $C(Q^2)$  from the available data (rather than from the Gross-Llewellyn Smith sum rule<sup>23</sup>), we find that use of  $\eta_1^{\text{BG}}$  and  $\eta_2^{\text{BG}}$  changes  $r_{53}$  from 1.35 to 1.42. Other parametrizations we tried lowered  $r_{53}$  to 1.15. Also with use of Eq. (5.8) but with a 100% error assigned to extrapolated points,  $r_{53}$  changes from 1.35 to  $1.42 \pm 0.27$ . We conclude that it is important to assign large errors (at least 50%) to extrapolated points.

With our grids there are five points of overlap between the SLAC and CDHS data. The average value of the ratio of SLAC to CDHS data is  $1.13 \pm 0.10$  (the error is consistent with the SLAC and CDHS systematic errors). If all SLAC data are divided by 1.13 before they are combined with CDHS data, one obtains  $d_5/d_3 = 1.30$  instead of 1.35. Part of the difference in normalization may be due to different assumptions about the relation between  $2xF_1$  and  $F_2$  (see Eq. 2.2). For the CDHS data the Callan-Gross relation,<sup>15</sup>  $2xF_1 = F_2$ , was assumed whereas for SLAC data  $R = 0.21 \Rightarrow 2xF_1/F_2 = (1 + 4M^2x^2/Q^2)/1.21$ . If one uses the Callan-Gross relation for SLAC data, then the relative normalization is  $1.065 \pm 0.10$  and  $d_5/d_3 = 1.40$  instead of 1.35. However, we must emphasize that SLAC data are not consistent with  $2xF_1 = F_2$ , so results based on assuming it are not meaningful. The errors introduced by these problems we believe are covered by our quoted error bars.

Our final observation with regard to moments concerns the significance of the agreement between the results of theory and experiment for  $r_{ij}$ . We have considered<sup>2</sup> for the sake of argument the extreme case where almost all scaling

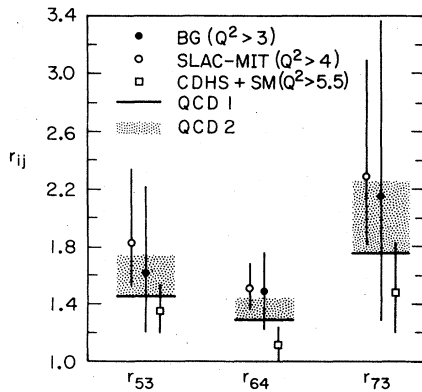


FIG. 10. Values of  $r_{ij} \equiv d_i/d_j$  for various combinations of  $i$  and  $j$  from the SLAC-MIT data (Ref. 5), the BEBC-Gargamelle (BG) data (Ref. 13), and a combination of the SLAC-MIT data (Ref. 5) and the CDHS data (Ref. 13). For SLAC-MIT alone we used  $F_2^{ep} - F_2^{en}$ , whereas in the combined fit, we used SLAC-MIT data for  $F_2^{ed}$  (with  $x > 0.4$ ).

violation comes from higher-twist terms (i.e.,  $\Lambda \approx 0$ ). There are no unequivocal calculations in QCD of the form of higher-twist terms, but from the quark-counting approach,<sup>19</sup> one can argue that the following parametrization of higher-twist terms in moments is reasonable:

$$M_2^{NS}(i, Q^2) = K_i \left[ 1 + \frac{a^2 i}{Q^2} + \frac{b^4 i^2}{Q^4} \right]. \quad (5.9)$$

If one obtains an effective  $r_{ij}$  by plotting  $\ln M_2(i, Q^2)$  versus  $\ln M_2(j, Q^2)$  and measuring the slope, one finds<sup>2</sup> surprisingly that the effective  $r_{ij}$  from Eq. (5.9) is consistent with the data as long as  $0 < a, b \leq 1$  GeV. The  $Q^2$  dependence of the moments requires, of course, particular choices for  $a$  and  $b$ . This result occurs because Eq. (5.9) gives  $r_{ij} \equiv d_i/d_j \approx i/j$  which is similar to both the data and QCD.

## VI. CONCLUSIONS

When the logarithmic scaling violation from the strong coupling constant and the power-law scaling violation from higher-twist operators are considered together, we find that (1) it is not possible with SLAC data alone to obtain an unequivocal test of QCD, (2) the value of  $\Lambda$  could be a factor of 2

smaller than what is found when higher-twist effects are ignored, (3) the values of the ratios of anomalous dimensions may reflect the presence of higher-twist terms, and (4) it is possible that the magnitude of  $R$  can be understood in the context of QCD when higher-twist terms are included.

It may be quite useful for muon experiments to combine their data with that from SLAC, but only if comparisons are made in overlap regions and if the results are not significantly affected by normalization differences.

Finally, it should be emphasized that all the SLAC data for  $F_2(x, Q^2)$  are entirely consistent with the predictions of QCD.

## ACKNOWLEDGMENTS

We would like to acknowledge valuable conversations with R. Blankenbecler, S. Brodsky, A. Buras, D. Coward, H. DeStaebler, J. Ellis, H. Georgi, F. Gilman, V. Korbel, M. Mestayer, M. Mugge, A. Para, D. Perkins, D. Politzer, D. Schlatter, W. Scott, and R. Taylor. This work was supported by the Department of Energy under Contract Nos. DE-ACO3-76SF00515 and E(11-1)3230.

<sup>1</sup>H. D. Politzer, Phys. Rev. Lett. **30**, 1346 (1973); D. J. Gross and F. Wilczek, *ibid.* **30**, 1343 (1973); Phys. Rev. D **8**, 3633 (1973); D **9**, 980 (1974); A. Zee, F. Wilczek, and S. B. Treiman, *ibid.* **10**, 2881 (1974); H. Georgi and H. D. Politzer, *ibid.* **9**, 416 (1974); S. Weinberg, Phys. Rev. Lett. **31**, 494 (1973).

<sup>2</sup>L. F. Abbott and R. M. Barnett, Ann. Phys. (N.Y.) **125**, 276 (1980); L. F. Abbott, in *High-Energy Physics in the Einstein Centennial Year*, proceedings of Orbis Scientiae, 1979, Coral Gables, edited by A. Perlmutter, F. Krausz, and L. F. Scott (Plenum, New York, 1979); R. M. Barnett, in *Quantum Chromodynamics*, proceedings of the Summer Institute on Particle Physics, SLAC, 1979, edited by Anne Mosher (SLAC, Stanford, 1980); W. B. Atwood, *ibid.*

<sup>3</sup>V. Baluni and E. Eichten, Phys. Rev. Lett. **37**, 1181 (1976); Phys. Rev. D **14**, 3045 (1976); G. C. Fox, Nucl. Phys. **B131**, 107 (1977); **B134**, 269 (1978); A. J. Buras and K. J. F. Gaemers, *ibid.* **B132**, 249 (1978); P. W. Johnson and W. T. Tung, *ibid.* **B121**, 270 (1977); M. M. Glück and E. Reya, *ibid.* **B156**, 456 (1979); D. W. Duke and R. G. Roberts, Phys. Lett. **85B**, 289 (1979); L. Baulieu and C. Kounnas, Nucl. Phys. **B155**, 429 (1979); C. Avilez *et al.*, Strasbourg Report No. CRN/HE-79-11 (unpublished); E. Reya, Report No. DESY-79/30, 1979 (unpublished); I. A. Schmidt and R. Blankenbecler, Phys. Rev. D **16**, 1318 (1977). See also Ref. 6. QCD analyses also appear in experimental papers, Refs. 13 and 14.

<sup>4</sup>K. Wilson, Phys. Rev. **179**, 1499 (1969); C. G. Callan,

Jr., in *Proceedings of the International School of Physics "Enrico Fermi" Course 54, Developments in High-Energy Physics*, edited by R. Gatto (Academic, New York, 1972); H. D. Politzer, in *Deeper Pathways in High Energy Physics*, proceedings of Orbis Scientiae, 1977, Coral Gables, Florida, edited by A. Perlmutter and L. F. Scott (Plenum, New York, 1977), p. 621; I. A. Schmidt and R. Blankenbecler, Phys. Rev. D **16**, 1318 (1977); S. Gottlieb, Nucl. Phys. **B139**, 125 (1978); K. Bitar, P. W. Johnson, and W.-K. Tung, Phys. Lett. **83B**, 114 (1979).

<sup>5</sup>Experiments used from the SLAC and MIT-SLAC collaborations, E49a: J. S. Poucher *et al.*, Phys. Rev. Lett. **32**, 118 (1974); J. S. Poucher, Ph.D. thesis, MIT, 1971 (unpublished); E49b: A. Bodek *et al.*, Report No. SLAC-PUB-1327 (unpublished); A. Bodek, Ph.D. thesis, MIT LNS Report No. COO-3069-116, 1972 (unpublished); E. M. Riordan, Ph.D. thesis, MIT LNS Report No. COO-3069-176, 1972 (unpublished); E89-1: W. B. Atwood, Ph.D. thesis, SLAC Report No. 185 (unpublished); E89-2: M. D. Mestayer, Ph.D. thesis, SLAC Report No. 214 (unpublished); E87: E. M. Riordan *et al.*, Report No. SLAC-PUB-1634 (unpublished); A. Bodek *et al.*, Phys. Rev. D **20**, 1471 (1979). These data are available on request from W. B. Atwood at SLAC.

<sup>6</sup>E. G. Floratos, D. A. Ross, and C. T. Sachrajda, Nucl. Phys. **B129**, 66 (1977) [**B139**, 545(E) (1978)]; Nucl. Phys. **B152**, 493 (1979); Phys. Lett. **80B**, 269 (1979). W. A. Bardeen, A. J. Buras, D. W. Duke, and T. Muta,

- Phys. Rev. D **18**, 3998 (1978); W. A. Bardeen and A. J. Buras, Phys. Lett. **86B**, 61 (1979); **90B**, 485(E) (1980); for a review, see A. J. Buras, Rev. Mod. Phys. **52**, 199 (1980).
- <sup>7</sup>M. Moshe, Phys. Rev. Lett. **43**, 1851 (1979).
- <sup>8</sup>O. Nachtmann, Nucl. Phys. **B63**, 237 (1973); H. Georgi and H. D. Politzer, Phys. Rev. D **14**, 1829 (1976); Phys. Rev. Lett. **36**, 1281 (1976); S. Wandzura, Nucl. Phys. **B122**, 412 (1977).
- <sup>9</sup>A. De Rújula, H. Georgi, and H. D. Politzer, Phys. Lett. **64B**, 428 (1977); Ann. Phys. (N.Y.) **103**, 315 (1977); E. Bloom and F. Gilman, Phys. Rev. Lett. **25**, 1140 (1970); R. Barbieri, J. Ellis, M. K. Gaillard, and G. G. Ross, Phys. Lett. **64B**, 171 (1976); Nucl. Phys. **B117**, 50 (1976); R. K. Ellis, R. Petronzio, and G. Parisi, Phys. Lett. **64B**, 97 (1976); D. J. Gross, S. B. Treiman, and F. A. Wilczek, Phys. Rev. D **15**, 2486 (1977).
- <sup>10</sup>G. Altarelli and G. Parisi, Nucl. Phys. **B126**, 298 (1977); Yu. L. Dokshitser, D. I. Dyakonov, and S. I. Troyan, Report No. SLAC-TRANS-0183, translated from Proceedings of the 13th Leningrad Winter School on Elementary Particle Physics, 1978, pp. 1-89 (unpublished); J. Kogut and L. Susskind, Phys. Rev. D **9**, 697 (1974); **9**, 3391 (1974); G. Parisi, Phys. Lett. **43B**, 207 (1973); D. J. Gross, Phys. Rev. Lett. **32**, 1071 (1974); C. H. Llewellyn Smith, Report No. OXFORD-TP 47/78, 1978 (unpublished); W. R. Frazer and J. F. Gunion, Phys. Rev. D **19**, 2447 (1979).
- <sup>11</sup>A. De Rújula, H. Georgi, and H. D. Politzer, Ann. Phys. (N.Y.) **103**, 315 (1977); H. D. Politzer, Nucl. Phys. **B122**, 237 (1977).
- <sup>12</sup>M. D. Mestayer, Ph.D. thesis, SLAC Report No. 214 (unpublished); E. M. Riordan *et al.*, Report No. SLAC-PUB-1634 (unpublished); A. Bodek *et al.*, Phys. Rev. D **20**, 1471 (1979).
- <sup>13</sup>P. C. Bosetti *et al.* BEBC-Gargamelle, Nucl. Phys. **B142**, 1 (1978); we thank W. Scott for providing us with up-to-date data from BEBC-Gargamelle; J. G. H. DeGroot *et al.* (CDHS), Phys. Lett. **82B**, 292 (1979); **82B**, 456 (1979); Z. Phys. C **1**, 142 (1979).
- <sup>14</sup>B. A. Gordon *et al.* (Chicago-Harvard-Illinois-Oxford), Phys. Rev. D **20**, 2645 (1979); R. C. Ball *et al.*, Phys. Rev. Lett. **42**, 866 (1979); B. A. Gordon *et al.*, *ibid.* **41**, 615 (1978); C. Chang *et al.*, *ibid.* **35**, 901 (1975).
- <sup>15</sup>C. G. Callan and D. J. Gross, Phys. Rev. Lett. **22**, 156 (1969).
- <sup>16</sup>W. B. Atwood and G. B. West, Phys. Rev. D **7**, 773 (1973).
- <sup>17</sup>L. L. Frankfurt and M. I. Strikman, Leningrad, INP report, 1976 (unpublished).
- <sup>18</sup>S. Stein *et al.*, Phys. Rev. D **12**, 1884 (1975); also see H. D. Politzer, Nucl. Phys. **B122**, 237 (1977) for comment.
- <sup>19</sup>S. J. Brodsky and G. Farrar, Phys. Rev. Lett. **31**, 1153 (1973); Phys. Rev. D **11**, 1309 (1975); R. Blankenbecler and S. J. Brodsky, *ibid.* **10**, 2973 (1974); I. A. Schmidt and R. Blankenbecler, *ibid.* **16**, 1318 (1977); H. D. Politzer, in *Deeper Pathways in High-Energy Physics*, proceedings of Orbis Scientiae, 1977, Coral Gables, edited by A. Perlmutter and L. F. Scott (Plenum, New York, 1977), p. 621.
- <sup>20</sup>We thank H. Georgi for suggesting this figure.
- <sup>21</sup>L. F. Abbott, E. L. Berger, R. Blankenbecler, and G. L. Kane, Phys. Lett. **88B**, 157 (1979).
- <sup>22</sup>A. J. Buras and K. J. F. Gaemers, Nucl. Phys. **B132**, 249 (1978).
- <sup>23</sup>D. J. Gross and C. H. Llewellyn Smith, Nucl. Phys. **B14**, 337 (1969).